Egyptian Geophysical Society
EGS Journal, Vol. 11, No. 1, 137-149 (2013)

SHALLOW GEOPHYSICAL INVESTIGATIONS FOR ENGINEERING-GEOLOGICAL PURPOSES AT GEBEL LIBNI CEMENT FACTORY, AL-ARISH AREA, SINAI PENINSULA, EGYPT

A.K. El-Werr

Associate professor, Geophysics Department, Faculty of Science, Ain Shams University, Egypt

فحوصات جيوفيزيقية ضحلة للأغراض الجيولوجية–الهندسية بموقع مصنع أسمنت جبل لبنى، منطقة العريش، شبه جزيرة سيناء، مصر

الخلاصة: تم انجاز عمل القياسات الجيوفيزيقية السطحية باستخدام طرق الانكسار السيزمى الضحل والكهرومغناطيسية منخفضة التردد للموقع المقترح لانشاء مصنع أسمنت جبل لبنى وذلك بهدف تقييم الخواص الجيوتقنية لمواد قطاع التربة لاستخدامها فى الأغراض الهندسية وكذلك تحديد ما اذا كان هناك كهوف ومياه جوفية ضحلة أم لا. وأظهرت نتائج تفسير البيانات من الطريقتين قطاع تربة مكون من أربعة طبقات ومقطوع بصدع عادى وممتد فى المنطقة فى الاتجاه الشمال الغربى–الجنوب الشرقى ويرمى فى اتجاه الجنوب الغربى. واتضح وجود تغييرات كبيرة فى كل من سمك الطبقات وسرعتها السزمية وكثافة التيار الكهرومغناطيسى المكافئ لكل طبقة. لذلك تم أيضا حساب المدلولات الجيوتقنية لطبقتى الأساسات الأولى والثانية لترجمتها هندسيا. واتضح أن مواد قطاع التربة لهذه الطبقات مناسبة للانشاءات الهندسية خاصة فى الجزء الجنوبى من منطقة الدراسة التى تتميز بقدرة تحمل أكثر من الجزء الشمالى شرط أن تنشأ على أحد جانبى الصدع وليست قاطعة له. ولم يلاحظ وجود كهوف ولا مياه جوفية ضحلة حتى عمق ٤٠ متر.

ABSTRACT: *Surface geophysical measurements using shallow seismic refraction and very low frequency electromagnetic (VLF-EM) methods have been carried out at a proposed site for construction of Gebel Libni Cement Factory, Sinai, aiming at the evaluation of the geotechnical properties of its soil materials for engineering purposes and the detection of cavernous structures and shallow groundwater. The results of data interpretation provide four-layer soil profile intersected by a NW-SE trending normal fault with a throw toward the southwest. The thickness, seismic velocity and EM equivalent current-density are very variable within each layer. The geotechnical parameters for the first and second layers were also calculated. The soil profile materials are suitable for any kind of constructions, particularly in the southern part of the study area, which is more competent than the northern part. However, the fault trace should not cross any kind of structure, i.e. the load of the engineering structure must be constructed on one side of the fault trace. Neither cavernous structures nor shallow groundwater was observed till 40 m depth range*

***Keywords**: Seismic refraction, VLF-EM, Gebel Libni, Al-Arish, engineering purposes.*

INTRODUCTION

Gebel Libni area is located in the northeastern part of Sinai Peninsula, to the northwest of Gebel El-Halal. It is accessible through roads coming from Ismaellia, Al-Arish and El-Hassana (Fig. 1). Gebel Libni is a relatively small oval-shaped massive hill extending in the NE–SW direction. Its long axis is 10 km length, whereas its short axis measures 7 km near its center, covering an area of about 70 km², and rises up to 463 m above sea level. The bulk of Gebel Libni is made up of Upper Cretaceous limestone beds in an antiform structure, dipping 10–30° away from the core in all directions. The proposed factory site lies to the southeast of Gebel Libni, south of the Ismaellia-El-Hassana asphaltic road, and north of Gebel El-Gendi. Fig. 2 represents a cross-section from the south of Gebel Libni to Gebel El-Gendi, passing through the proposed factory site. It roughly traces the subsurface geology beneath the gravel–sand plain. Rock units are obviously dipping southward, as a continuation of Gebel Libni anticlinal structure, but gently turning away to a synclinal structure in an area south of Gebel El-Halal. The white massive and thick-bedded bioclastic limestone of the Upper Cretaceous Libni Member is exposed at higher altitudes over Gebel Libni anticlinal structure. This can be quarried as basic raw materials for any planned cement factories in the area. At Gebel El-Gendi, the near-surface layers become almost horizontal, some of which crop out more than 10 m above the ground surface. These layers are of Early Eocene age and composed mainly of chalky, argillaceous and marly limestone.

In the present study, shallow seismic refraction and very low frequency electromagnetic (VLF-EM) methods have been carried out aiming at the evaluation of the geotechnical properties of the soil materials, which are very important for construction of any engineering project. Mencl (1966) stated that, "the object of engineering-geological investigations of soil and/or rock materials is to obtain engineering information standing behind their geological properties, such as bulk density, strength, deformability, bearing capacity, …etc". This information is usually needed for civil engineering purposes. The engineering-geological characters of soil and rocks are the result of their genesis, mineral composition and texture, i.e. their petrogenesis and petrography (Kelly and Mares, 1993).

The principal task of shallow seismic refraction in this work is the assessment of the engineering-geological or geotechnical properties as well as the physical state of the soil materials through the determination of some physical parameters, such as velocity of elastic wave propagation, while VLF-EM method is to effectively map the underlying clays, detect the cavernous structures and investigate the groundwater regime.

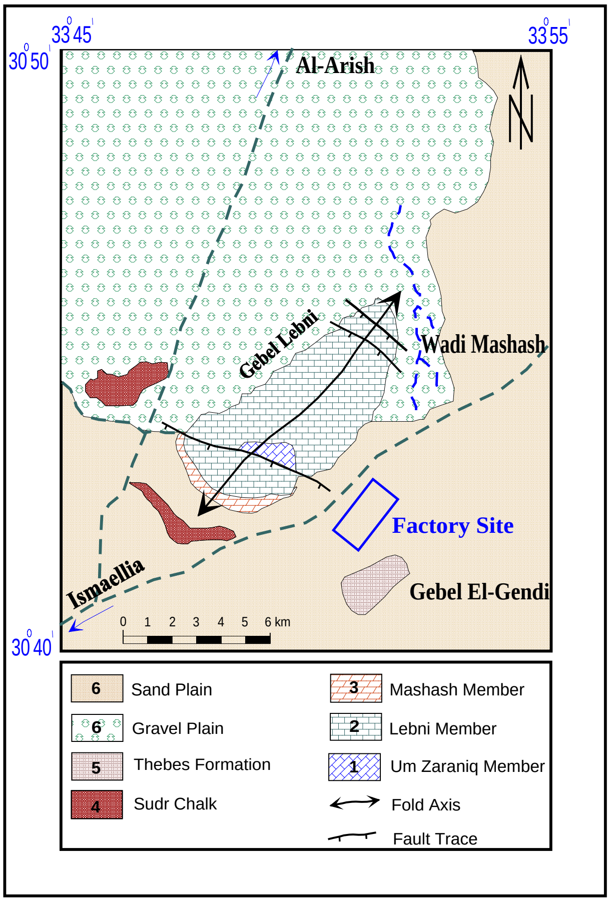

Fig. 1: Simplified geological map of Gebel Libni area.

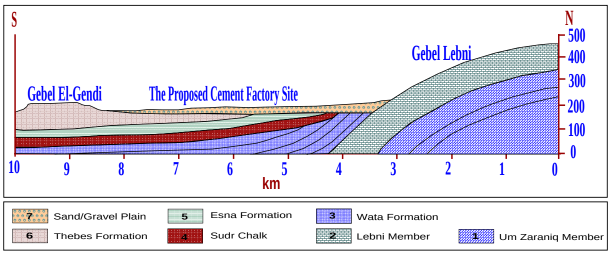

Fig. 2: Geological cross-section running from the south of Gebel Libni to Gebel El-Gendi, passing through the proposed cement factory site

GEOPHYSICAL DATA ACQUISITION

1. Shallow Seismic Refraction Data Acquisition:

During seismic refraction field surveys a twenty-four channel SmartSeis Geometrics Seismograph was used. Twenty-four vertical component geophones with natural frequency of 14 Hz were used to detect the compressional seismic waves and twelve horizontal component geophones with natural frequency of 14 Hz were used to detect the shear seismic waves. Twenty-three seismic profiles were acquired in the study area, as shown in the seismic profile location map (Fig.3). In-line geophone spread was used in this survey with two end-on shots and one split spread shot. The length of each seismic spread was 250 m, with 10 m geophone interval. The source of seismic energy was a sledgehammer hitting vertically on a striker plate laid on the ground surface. Stacking was always done through several impacts for signal enhancement till a good data quality is reached. Selected example of shot records is shown in Fig. 4 with record length of 256 ms.

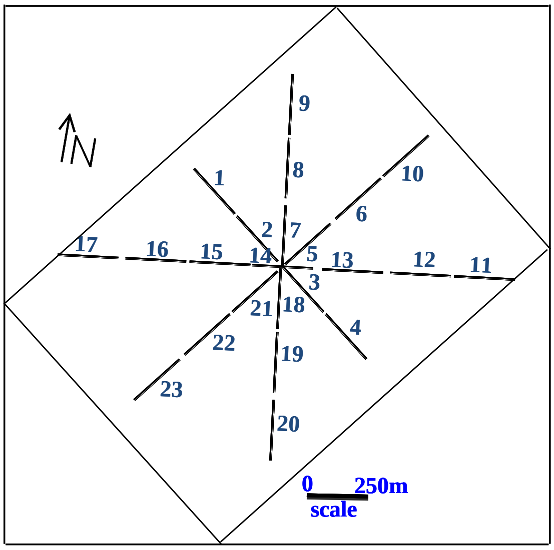

Fig. 3: Seismic profile location map.

2. VLF-EM Data Acquisition:

The very low frequency-electromagnetic technique uses radiations generated by remote powerful radio-transmitters. These radio-transmitters are distributed allover the world for military communication purposes operating at the frequency range of 15-30 kHz and emitting continuously either superimposed frequency modulated waves or occasionally chopped un-modulated "Morse code" (Watt, 1967; West and Macnae, 1991; and Turberg et al., 1994). The profile direction in the VLF-EM work is almost irrelevant and the subsurface conductor, which strikes towards the radio-transmitter, is well-coupled as the magnetic field is at right angle to it and the current can flow freely. Otherwise, the current flow would be restricted and reduces the strength of the secondary field (Turberg and Barker, 1996).

The VLF-EM field method is rather simple and can work as follows: the VLF receiver is tuned to a particular frequency of the selected radio-transmitter. The azimuth of the radio-transmitter is obtained by rotating a small induction coil around a vertical axis until the null position is found.

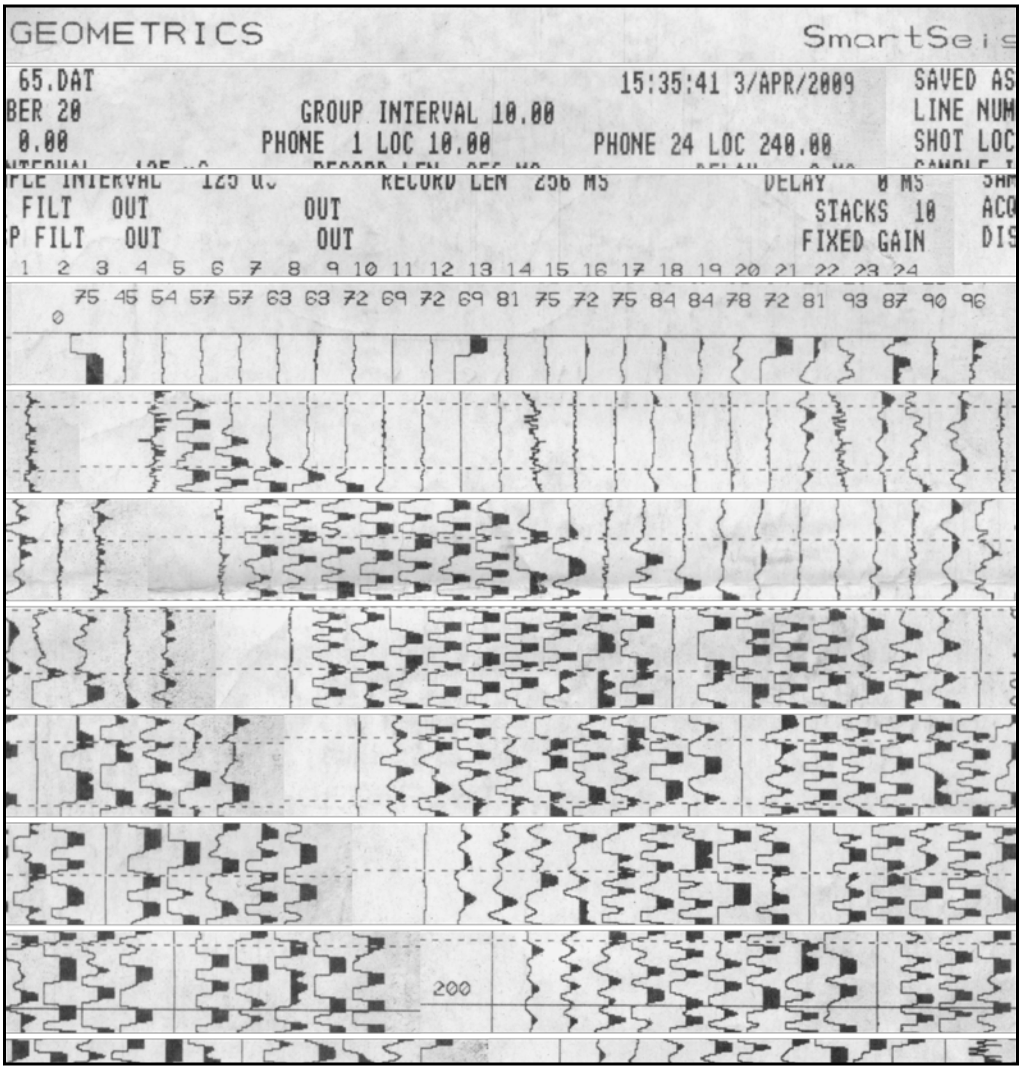

Fig. 4: Selected example of shot records.

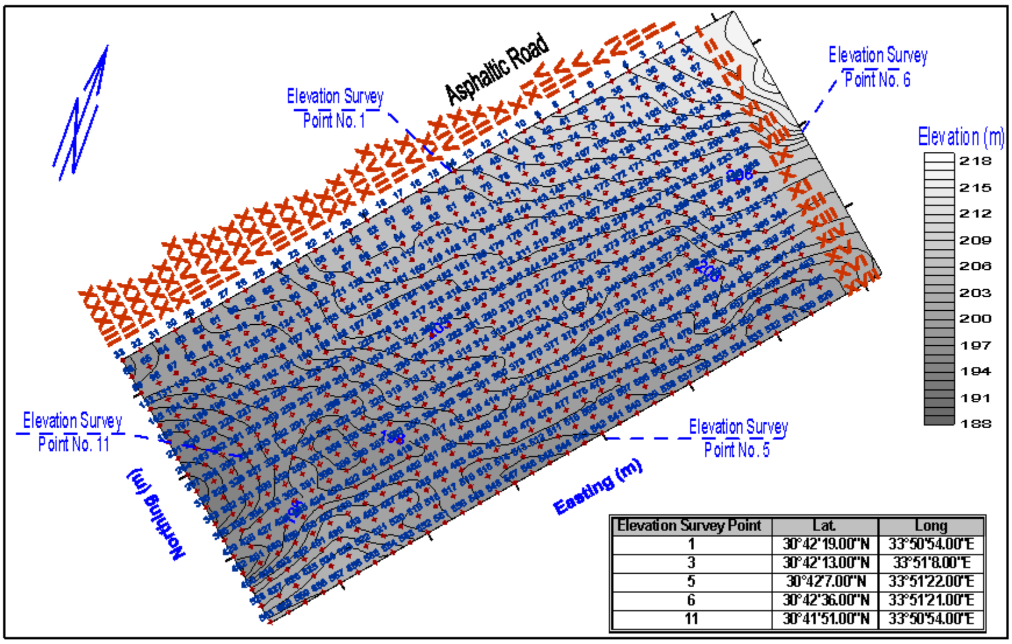

Elevation Survey Point	Lat.	Long
1	30°42'19.00"N	33°50'54.00"E
3	30°42'13.00"N	33°51'8.00"E
5	30°42'7.00"N	33°51'22.00"E
6	30°42'36.00"N	33°51'21.00"E
11	30°41'51.00"N	33°50'54.00"E

Fig. 5: VLF profile location map.

The coil is rotated around a horizontal axis at right angle to that azimuth, where both the in-phase (real) and out-phase (imaginary) components of the complex quantity "secondary/primary fields are noted.

Measurements are then performed along the surveyed profile at right-angle to that azimuth using only a single and well-defined frequency. The present measurements were carried out using the WADI^{TM} VLF–EM system of ABEM Instruments, Sweden) along forty profiles (seventeen longitudinal and thirty-three transverse) at the proposed factory site of Gebel Libni Cement Factory, Al-Arish, North Sinai (Fig. 5). The spacing between the measuring points was 50 m, and the measuring profiles were also 50 m apart. The operating frequency was the powerful at 21.7 kHz at measuring azimuth 45^{o} N.

GEOPHYSICAL DATA INTERPRETATION

1. Seismic Refraction Data Interpretation:

Seismic refraction data interpretation is usually used for depth determination under the shot points and beneath each geophone and also for calculation of the true velocities for each investigated layer. Interpretational methods based on delay time, plus-minus, generalized reciprocal time and ray-tracing are well explained in literature, (e.g. Hagedoorn, 1959; Redpath, 1973; Palmer, 1980, 1981 & 1986; Zhu and McMechan, 1988; Palmer, 1991 & 2000; Matsuoka et al., 2000; Palmer, 2001 & 2003 and Palmer and Jones, 2003). The collected travel times along each interpreted profile were inverted into seismic velocity-depth models using seismic refraction inversion software called "WIN SIP". This software calculates the subsurface layer depths and velocities. Four sedimentary layers have been identified in the suggested geoseismic cross sections (Fig. 6) in the depth range of about 50 m, with widely variable layer thicknesses and velocities. Another geoseismic cross section reflects a normal fault with a throw toward the southwest direction (Fig. 7). This fault is directed toward the NW-SE and observed in profile numbers 5, 8 and 13, as shown in the fault location map (Fig. 8).The soil profile is represented by the following layers that are confirmed by the borehole drilling results: Layer 1: topsoil silty clayey sand with gravel and limestone fragments. Layer 2: weathered limestone (highly fractured) with some partings of marl and clay. Layer 3: limestone (moderately fractured) highly intercalated with marl and clay. Layer 4: limestone (slightly fractured) with partings of marl and clay.

Seismic compressional wave (P-wave) velocity maps were established for the interpreted four layers showing a wide range of velocity variations. The topsoil P-wave velocity map (Fig. 9) reveals the existence of lower velocities of about 300 m/s at the eastern and northern parts of the study area representing silty clayey sand with gravel, while higher values up to 820 m/sec are occurred at the southern and western parts due to the occurrence of limestone fragments. The thickness of the first layer is ranged between 3 to 8 m. The P-wave velocity map of the second layer (Fig. 10) reflects the velocity range 1200-2000 m/s and the thickness range 8-26 m for weathered and highly fractured limestone with also higher values in the southern, southwestern and northeastern parts. The first layer and the uppermost part of the second one can be considered as foundation layers and they are very suitable for any kind of construction. The third and fourth layers (Figs. 11 and 12) exhibit seismic velocities in the range of 1750–2450 m/s and 1900-2900 m/s, respectively for the moderately and slightly fractured limestone with marl and clay intercalations. Seismic shear wave (S-wave) velocity maps were constructed for the first two layers (Figs. 13 and 14) showing lower values of the loose sediments at the eastern and northern parts, while higher velocities occupied the southern and western parts.

ENGINEERING-GEOLOGICAL CHARACTERISTICS:

In addition to the P- and S-wave velocities, the bulk densities of the first two foundation layers were calculated (Figs. 15 and 16) using the Gardner, et al. (1974) relation of the density (ρ) and P-wave velocity (***Vp***) for sediments as follows:

$$\boldsymbol{\rho = 1.62 + 0.00021 Vp} \quad (1)$$

Once we have these three physical properties (***ρ, Vp*** and ***Vs***), any engineering-geological property or geotechnical parameter can be calculated.

1- Dynamic Shear Modulus (*μ*):

The dynamic shear modulus was calculated for the first and second layers using Imai and Uoshimura(1975) equation as follows:

$$\mu = \rho\, V_s^{\,2} \quad (2)$$

Fig. 17 shows the dynamic shear modulus map of the first layer reflecting lower values in the eastern and northern parts, while higher values occupy the southern and western parts. The dynamic shear modulus map of the second layer is shown in Fig. 18 exhibiting also lower values in the eastern and northern parts, while higher values occupy the central and western parts.

2-Ultimate and Allowable Bearing Capacities:

The ultimate bearing capacity (**Q_{ult}**) was calculated using the shear wave velocity according to Abd El-Rahman et al. (1992) and the allowable bearing capacity was calculated according to Hoek (2000) as follows:

$$Q_{ult} = 10^{2.932(\log Vs - 1.45)} \quad (3)$$

$$Q_a = Q_{ult} / f \quad (4)$$

where: "**f**" is the factor of safety and its value is assumed to be 2 for these soil materials.

The ultimate bearing capacity is ranged from 1 to 23 kg/cm^2 for the first layer and it is ranged from 60 to 300 kg/cm^2 for the second layer, while the allowable bearing capacity is ranged from 0.5 to 11.5 kg/cm^2 for the first layer and it is ranged from 30 to 150 kg/cm^2 for the second foundation layer, as shown in Figs. 19 through 22.

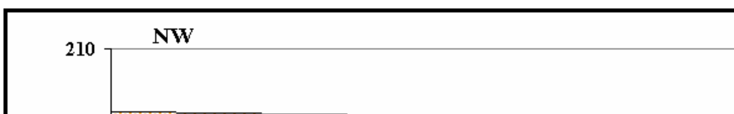

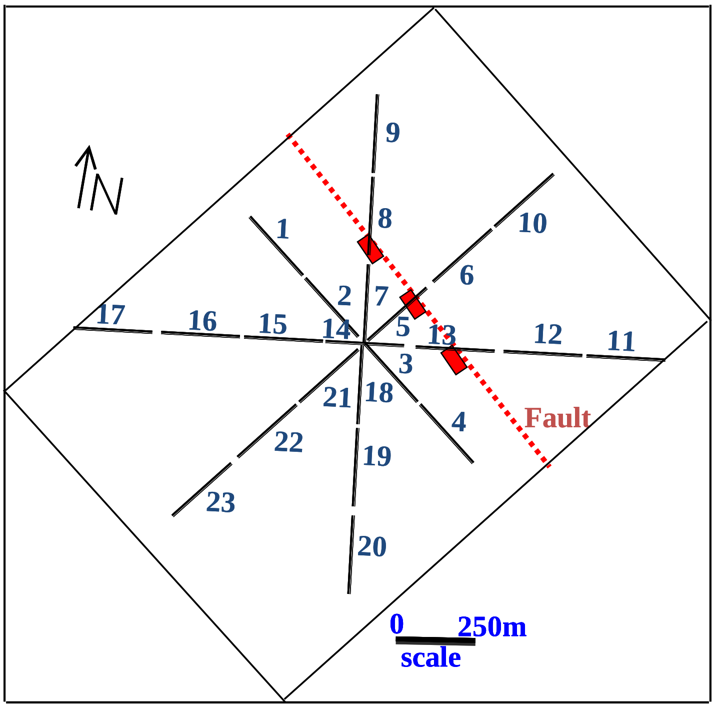

Fig. 8: A fault location map.

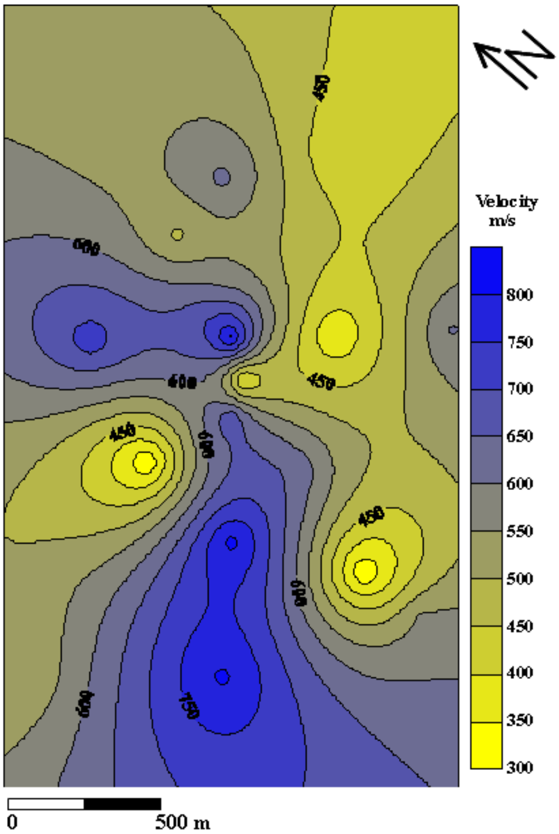

Fig. 9: First layer P-wave velocity map.

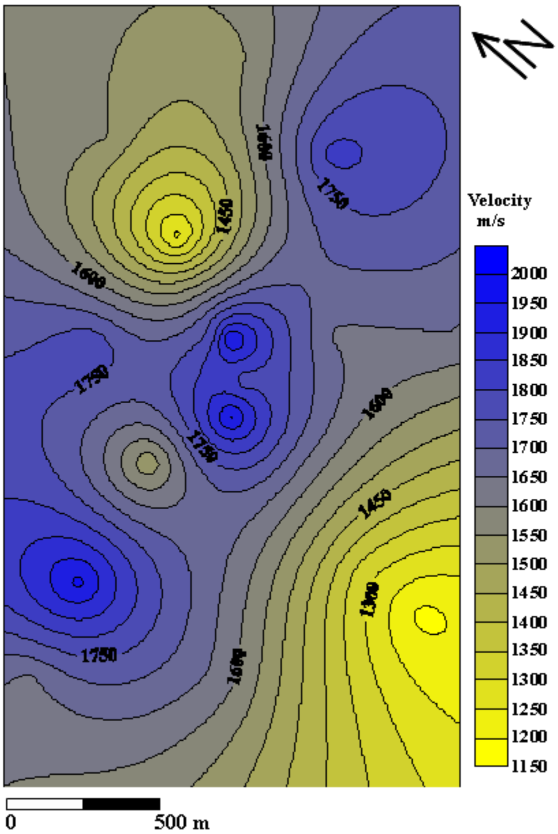

Fig. 10: Second layer P-wave velocity map.

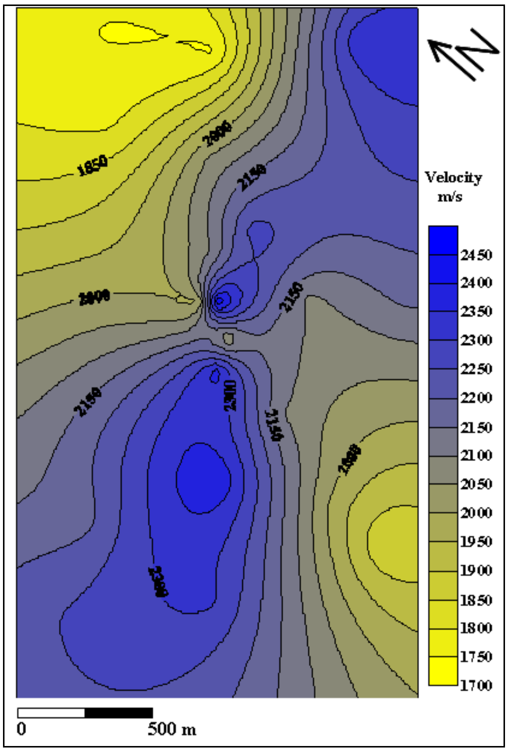

Fig. 11: Third layer P-wave velocity map.

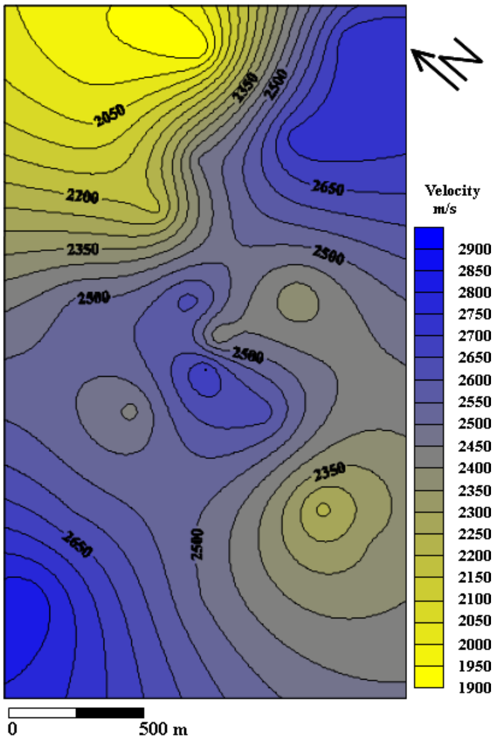

Fig. 12: Fourth layer P-wave velocity map.

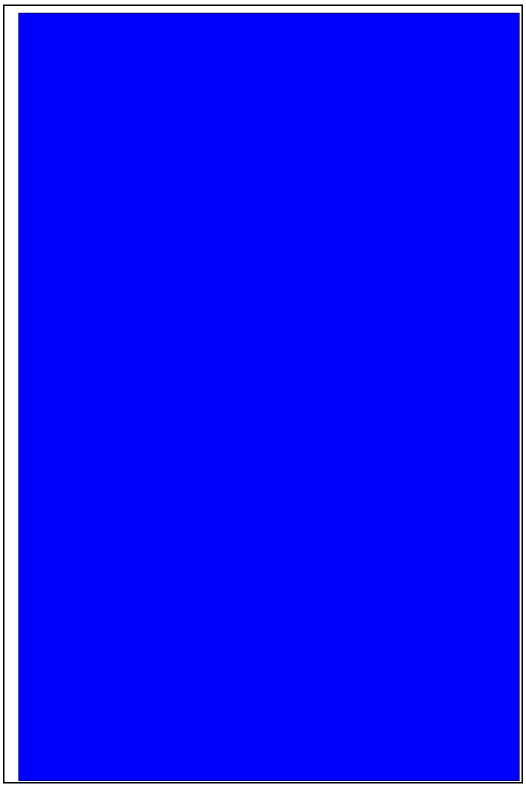

Fig. 13: First layer S-wave velocity map.

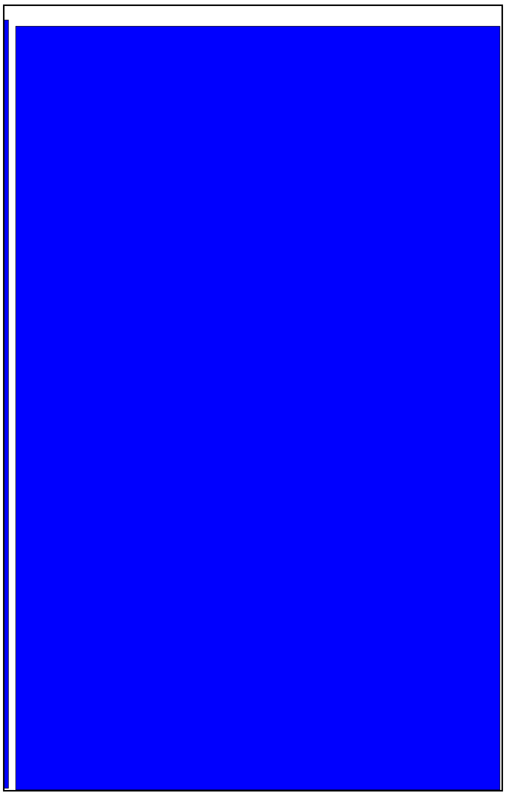

Fig. 14: Second layer S-wave velocity map.

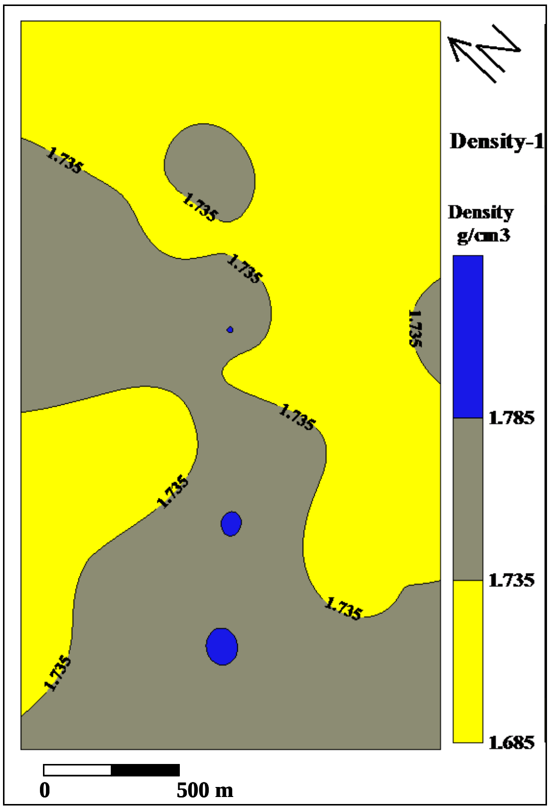

Fig. 15: First layer density map.

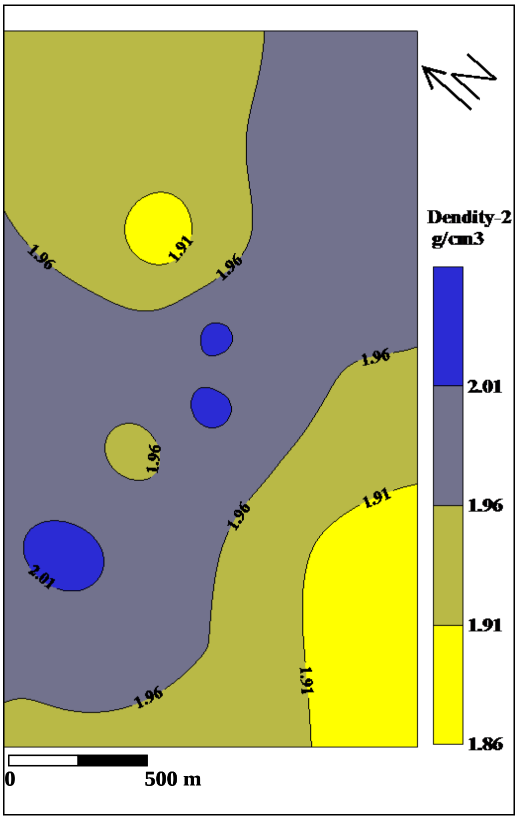

Fig. 16: Second layer density map.

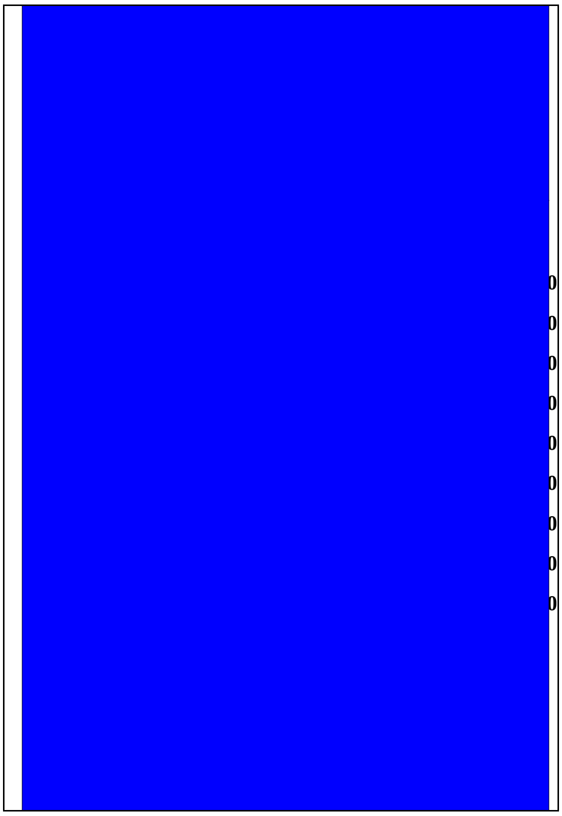

Fig. 17: First layer shear modulus map.

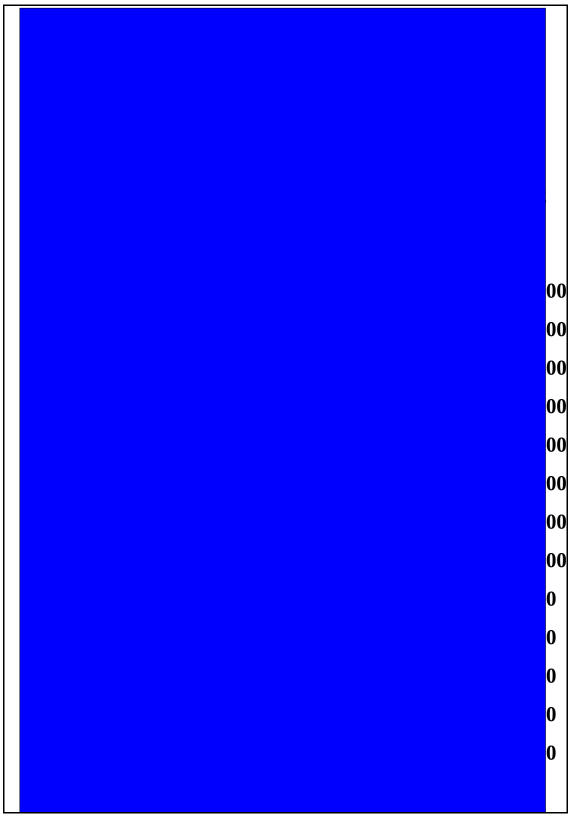

Fig. 18: Second layer shear modulus map

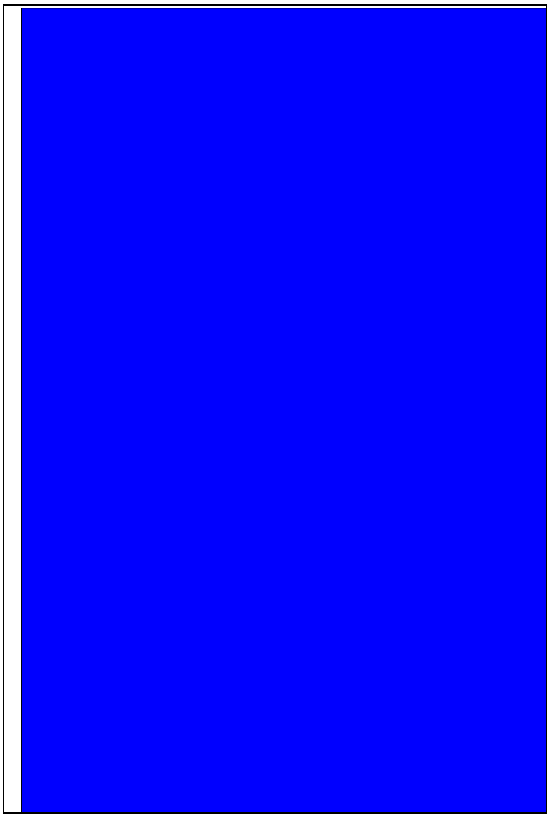

Fig. 19: First layer ultimate bearing capacity.

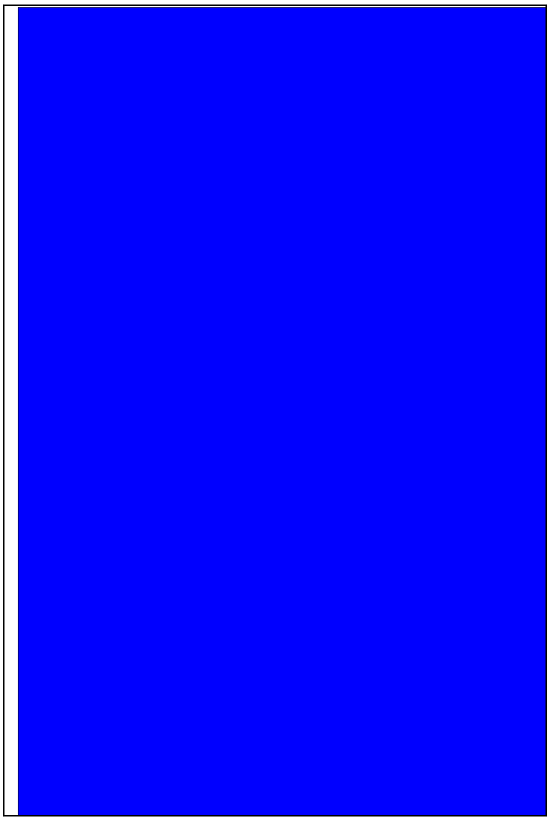

Fig. 20: Second layer ultimate bearing capacity.

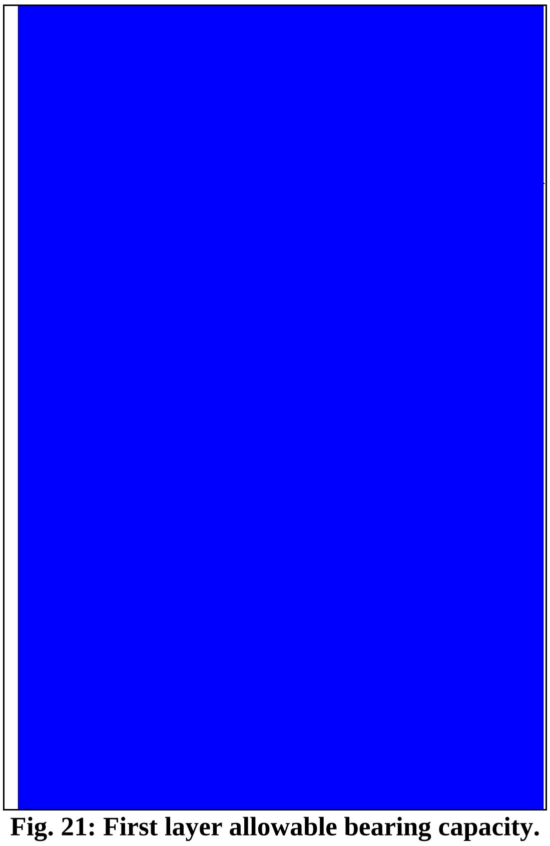

Fig. 21: First layer allowable bearing capacity.

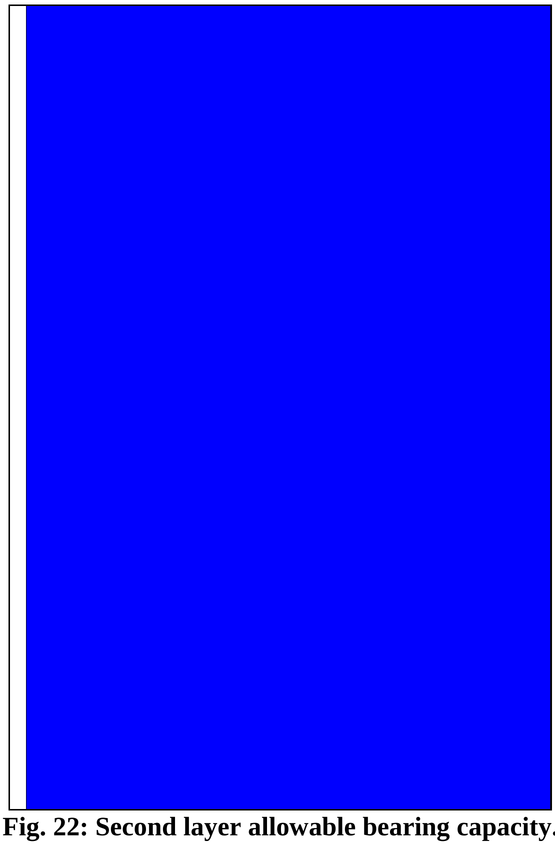

Fig. 22: Second layer allowable bearing capacity.

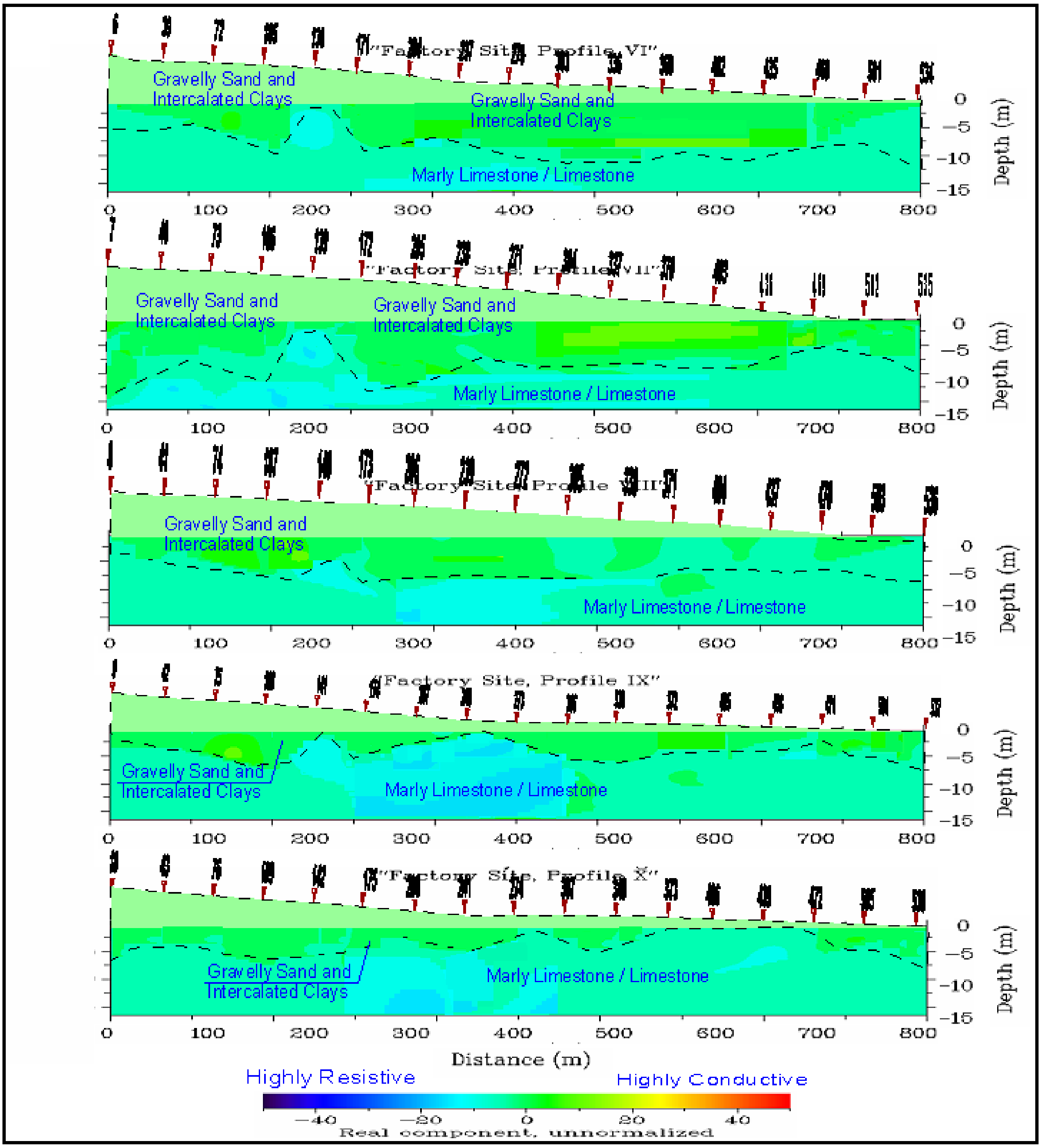

Fig. 23: Equivalent current-density sections along transverse profiles VI - X for the operating frequency 21.7 kHz, Hot colors represent conductive media, while cold colors represent resistive ones.

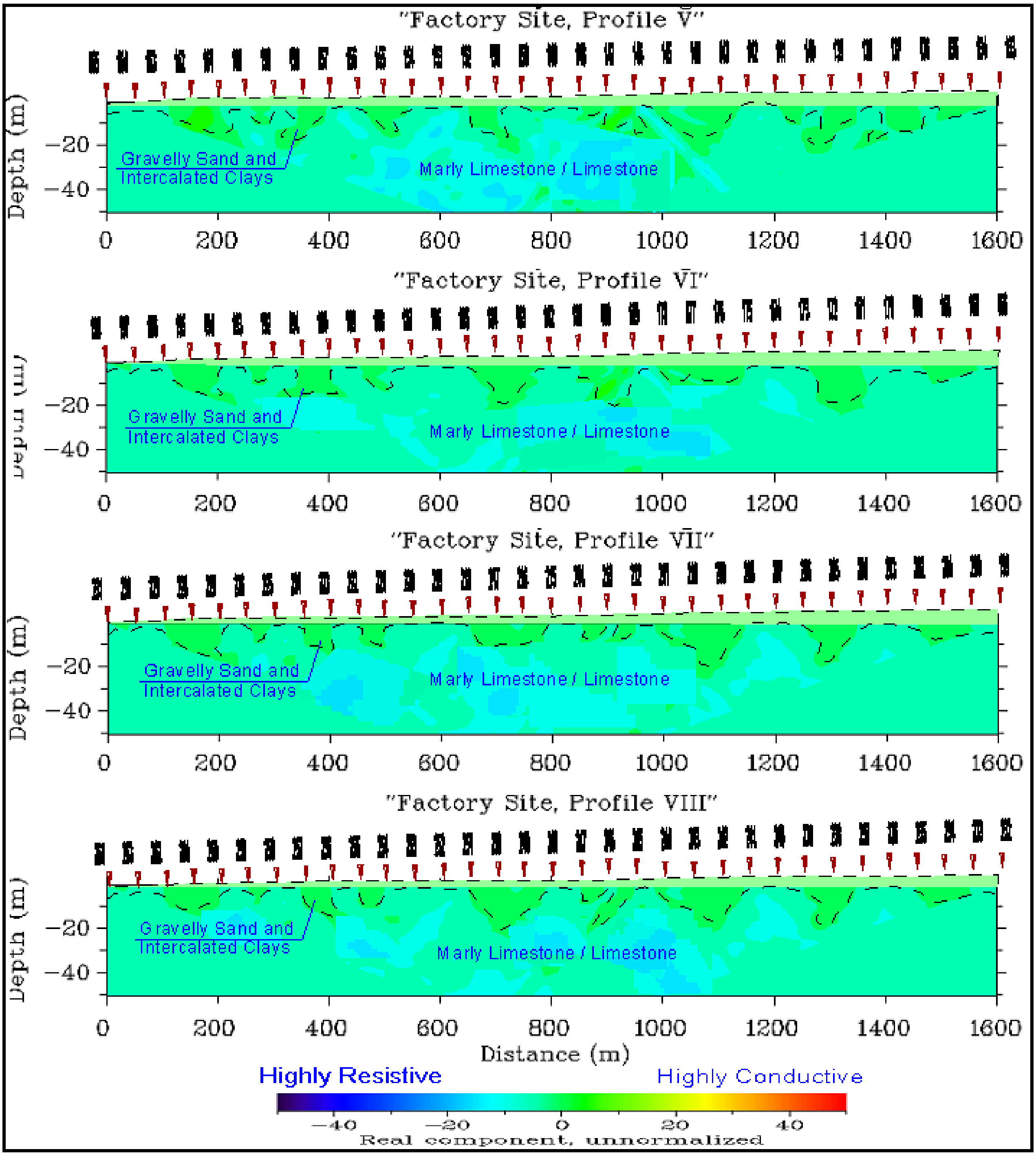

Fig. 24: Equivalent current-density sections along longitudinal profiles V - VIII.

2. VLF-EM Data Analysis

The VLF-EM technique is a very powerful tool for the detection of cavernous structures, when an extremely low equivalent current-density distribution is noticed in the contoured sections and for the detection of shallow groundwater regime, when an extremely high equivalent current-density distribution is found. Neither the first feature nor the second one was observed till 40 m depth range in the study area. However, the moderately conductive zone (dark green/pale green) represents the surface wadi deposits of the gravelly sands and intercalated clays of the topsoil layer and the moderately resistive zone (pale blue/pale green) represents the encountered fractured zones of the marly limestone/limestone of the second layer, while the more massive zones (blue/dark blue) indicate massive and very massive limestone of the third and fourth layers. These layer boundaries were roughly determined from the VLF equivalent current-density contoured sections, as shown in the transverse profiles VI through X (Fig. 23) and the longitudinal profiles V through VIII (Fig. 24).

CONCLUSIONS

Seismic refraction and very low frequency electromagnetic (VLF-EM) techniques have been used for the evaluation of the near-surface parts of the proposed site for construction of Gebel Libni Cement Factory, Al-Arish area, Sinai Peninsula, from an engineering point of view. Detection whether or not cavernous structures and shallow groundwater are present in the study, was also aimed. Four-layer soil profile was indicated from the results of seismic data interpretation intersected by a NW-SE normal fault throwing toward the southwest. Variable thicknesses and velocities were observed within this soil profile. The southern and central parts of the study area are more competent than the other parts and very suitable for any kind of constructions like, production lines of the cement factory taking into account the location of the fault trace, which should not cross any kind of an engineering structure.

The VLF-EM technique was proposed in this study, because it is very powerful tool for the detection of cavernous structures when an extremely low equivalent current-density distribution is noticed in the contoured sections and also for the detection of shallow groundwater regime, when an extremely high equivalent current-density distribution is found. However, moderately conductive zones are occurred in the shallower part of the soil profile, as shown in the colored sections (dark green/pale green) for the surface wadi deposits of the gravelly sands and intercalated clays of the topsoil layer, and the moderately resistive zones for the fractured marly limestone/limestone of the second layer (pale blue/pale green). While the more resistive zones (blue/dark blue) indicate massive/very massive limestone of the deeper layers. Neither cavernous structures nor shallow groundwater was observed till 40 m depth range.

REFERENCES

Abd El Rahman, M., Setto, I. and El-Werr, A., 1992, Inferring mechanical properties of the foundation materials at the 2nd industrial zone, Sadat city, from geophysical measurements: E.G.S. Proc. of the 10th Ann. Meet., March 1992, P. 50– 61.

Gardner, G. H. F., Gardner, L. W. and Gregory, A. R., 1974, Formation velocity and density- the diagnostic basics for stratigraphic traps: Geophysics, V. 39, P.770-780.

Hagedoorn, J. G., 1959: The plus-minus method for interpreting seismic refraction sections, Geophy. Prosp., v. 7, p. 158-181.

Hoek, E., 2000, Rock engineering, course notes**:** North Vancouver, B. C., Canada V 7 R 4X1.

Imai, T. and Yoshimura, M., 1975, The relation of mechanical properties of soils to P-and S-wave velocities for soil ground in Japan: Urawa Research Institute, OYO Corporation, RP- 447

Kelly, W. E., and Mares, S., 1993: Applied geophysics in hydrogeological and engineering practice, Elsevier science publishers B. V., 289 p.

Matsuoka, T., Taner, M. T., Hayashi, T., Ashida, Y., Watanabe, T., and Kusumi, H., 2000: Imaging of refracted waves by convolution, 70th Annual International Meeting, SEG.

Mencl, V., 1966: Mechanika zemin a skalnich hornin (Rock and soil mechanics), Academia, Prague, p. 329 (in Czech).

Palmer, D., 1980: The generalized reciprocal method of seismic refraction interpretation, Tulsa, Society of Exploration Geophysicists.

Palmer, D., 1981: An introduction to the generalized reciprocal method of seismic refraction interpretation, Geophysics, 46, 1508-1518.

Palmer, D., 1986: Refraction seismics: the lateral resolution of structure and seismic velocity, Geophysical Press.

Palmer, D., 1991: The resolution of narrow low-velocity zones with the generalized reciprocal method, Geophys. Prosp., 39, 1031-1060.

Palmer, D., 2000: Can new acquisition methods improve signal-to-noise ratios with seismic refraction techniques?, Exploration Geophysics, 31, 275-300.

Palmer, D., 2001: Imaging refractor with the convolution section, Geophysics, 66, 1582-1589.

Palmer, D., 2003: The shallow refraction method for the new millennium, Website, Dr. Derecke Palmer.htm, Science@UNSW.

Palmer, D. and Jones, L., 2003: Detailed refraction statics with the GRM and RCS, ASEG 16th Geophysical Conference and Exhibition, Adelaide, Expanded Abstracts.

Redpath, B. B., 1973: Seismic refraction exploration for engineering site investigation, National Technical Information Service.

Turberg, P. and Müller, I. and Flury, B., 1994: Hydrogeological investigation of porous environments by radio magnetotelluric-resistivity (RMT−R 12−240 kHz), Journal of Applied Geophysics, 31, 113−143.

Turberg, P. and Barker, R., 1996: Joint application of radiomagnetotelluric and electrical imaging surveys in complex subsurface environments, First Break, 14, 105−112.

Watt, A. D., 1967: VLF radio engineering. Pergamon Press, New York.

West, G. F. and Macnae, J. C., 1991: Physics of the electromagnetic induction exploration method, In Nabighian, M. N. (Ed.), Electromagnetic Methods in Applied Geophysics, Vol. 2A, Society of Exploration Geophysicists, Tulsa, 5−45.

Zhu, X. and McMechan, G., 1988: Ray tracing for surface source-to-surface recorder tomography, Center for lithospheric studies, University of Texas, Dallas.